Sub-micron absolute distance measurements in sub-millisecond times with dual free-running femtosecond Er fiber-lasers

Tze-An Liu,[1] Nathan R. Newbury,[2] and Ian Coddington[2,*]

[1]*Center for Measurement Standards, Industrial Technology Research Institute, 321, Sec.2, Kuang Fu Rd., Hsinchu 300, Taiwan*

[2]*National Institute of Standards and Technology, 325 Broadway, Boulder, CO 80305 USA*

**ian@nist.gov*

Abstract: We demonstrate a simplified dual-comb LIDAR setup for precision absolute ranging that can achieve a ranging precision of 2 μm in 140 μs acquisition time. With averaging, the precision drops below 1 μm at 0.8 ms and below 200 nm at 20 ms. The system can measure the distance to multiple targets with negligible dead zones and a ranging ambiguity of 1 meter. The system is much simpler than a previous coherent dual-comb LIDAR because the two combs are replaced by free-running, saturable-absorber-based femtosecond Er fiber lasers, rather than tightly phase-locked combs, with the entire time base provided by a single 10-digit frequency counter. Despite the simpler design, the system provides a factor of three improved performance over the previous coherent dual comb LIDAR system.

OCIS codes: (120.0120) Instrumentation, measurement, and metrology; (280.3640) Lidar; (120.0280) Remote sensing and sensors.

References and links

1. S. A. Diddams, "The evolving optical frequency comb," J. Opt. Soc. Am. B **27**(11), B51–B62 (2010).
2. N. R. Newbury, "Searching for applications with a fine-tooth comb," Nat. Photonics **5**(4), 186–188 (2011).
3. K. Minoshima and H. Matsumoto, "High-accuracy measurement of 240-m distance in an optical tunnel by use of a compact femtosecond laser," Appl. Opt. **39**(30), 5512–5517 (2000).
4. N. Schuhler, Y. Salvadé, S. Lévêque, R. Dändliker, and R. Holzwarth, "Frequency-comb-referenced two-wavelength source for absolute distance measurement," Opt. Lett. **31**(21), 3101–3103 (2006).
5. Y. Salvadé, N. Schuhler, S. Lévêque, and S. Le Floch, "High-accuracy absolute distance measurement using frequency comb referenced multiwavelength source," Appl. Opt. **47**(14), 2715–2720 (2008).
6. M. Cui, M. G. Zeitouny, N. Bhattacharya, S. A. van den Berg, H. P. Urbach, and J. J. M. Braat, "High-accuracy long-distance measurements in air with a frequency comb laser," Opt. Lett. **34**(13), 1982–1984 (2009).
7. K. N. Joo and S. W. Kim, "Absolute distance measurement by dispersive interferometry using a femtosecond pulse laser," Opt. Express **14**(13), 5954–5960 (2006).
8. M. Cui, M. G. Zeitouny, N. Bhattacharya, S. A. van den Berg, and H. P. Urbach, "Long distance measurement with femtosecond pulses using a dispersive interferometer," Opt. Express **19**(7), 6549–6562 (2011).
9. P. Balling, P. Kren, P. Masika, and S. A. van den Berg, "Femtosecond frequency comb based distance measurement in air," Opt. Express **17**(11), 9300–9313 (2009).
10. K. N. Joo, Y. Kim, and S. W. Kim, "Distance measurements by combined method based on a femtosecond pulse laser," Opt. Express **16**(24), 19799–19806 (2008).
11. S. Yokoyama, T. Yokoyama, Y. Hagihara, T. Araki, and T. Yasui, "A distance meter using a terahertz intermode beat in an optical frequency comb," Opt. Express **17**(20), 17324–17337 (2009).
12. I. Coddington, W. C. Swann, L. Nenadovic, and N. R. Newbury, "Rapid and precise absolute distance measurements at long range," Nat. Photonics **3**(6), 351–356 (2009).
13. J. Lee, Y. J. Kim, K. Lee, S. Lee, and S. W. Kim, "Time-of-flight measurement with femtosecond light pulses," Nat. Photonics **4**(10), 716–720 (2010).
14. H. Y. Xia and C. X. Zhang, "Ultrafast and Doppler-free femtosecondoptical ranging based on dispersivefrequency-modulated interferometry," Opt. Express **18**(5), 4118–4129 (2010).
15. M. Godbout, J. D. Deschênes, and J. Genest, "Spectrally resolved laser ranging with frequency combs," Opt. Express **18**(15), 15981–15989 (2010).
16. N. R. Doloca, K. Meiners-Hagen, M. Wedde, F. Pollinger, and A. Abou-Zeid, "Absolute distance measurement system using a femtosecond laser as a modulator," Meas. Sci. Technol. **21**(11), 115302 (2010).
17. F. Keilmann, C. Gohle, and R. Holzwarth, "Time-domain mid-infrared frequency-comb spectrometer," Opt. Lett. **29**(13), 1542–1544 (2004).

#151474 - $15.00 USD Received 21 Jul 2011; revised 22 Aug 2011; accepted 22 Aug 2011; published 7 Sep 2011

18. I. Coddington, W. C. Swann, and N. R. Newbury, "Coherent multiheterodyne spectroscopy using stabilized optical frequency combs," Phys. Rev. Lett. **100**(1), 013902 (2008).
19. P. Giaccari, J. D. Deschênes, P. Saucier, J. Genest, and P. Tremblay, "Active Fourier-transform spectroscopy combining the direct RF beating of two fiber-based mode-locked lasers with a novel referencing method," Opt. Express **16**(6), 4347–4365 (2008).
20. B. Bernhardt, A. Ozawa, P. Jacquet, M. Jacquey, Y. Kobayashi, T. Udem, R. Holzwarth, G. Guelachvili, T. W. Hänsch, and N. Picqué, "Cavity-enhanced dual-comb spectroscopy," Nat. Photonics **4**(1), 55–57 (2010).
21. J. D. Deschênes, P. Giaccarri, and J. Genest, "Optical referencing technique with CW lasers as intermediate oscillators for continuous full delay range frequency comb interferometry," Opt. Express **18**(22), 23358–23370 (2010).
22. I. Coddington, W. C. Swann, and N. R. Newbury, "Coherent linear optical sampling at 15 bits of resolution," Opt. Lett. **34**(14), 2153–2155 (2009).
23. G. Taurand, P. Giaccari, J. D. Deschênes, and J. Genest, "Time-domain optical reflectometry measurements using a frequency comb interferometer," Appl. Opt. **49**(23), 4413–4419 (2010).
24. M. Jiang, G. Sucha, M. E. Fermann, J. Jimenez, D. Harter, M. Dagenais, S. Fox, and Y. Hu, "Nonlinearly limited saturable-absorber mode locking of an erbium fiber laser," Opt. Lett. **24**(15), 1074–1076 (1999).
25. M. Guina, N. Xiang, and O. G. Okhotnikov, "Stretched-pulse fiber lasers based on semiconductor saturable absorbers," Appl. Phys. B **74**(9), S193–S200 (2002).
26. I. Hartl, G. Imeshev, M. E. Fermann, C. Langrock, and M. M. Fejer, "Integrated self-referenced frequency-comb laser based on a combination of fiber and waveguide technology," Opt. Express **13**(17), 6490–6496 (2005).
27. J. J. McFerran, L. Nenadovic, W. C. Swann, J. B. Schlager, and N. R. Newbury, "A passively mode-locked fiber laser at 1.54 mum with a fundamental repetition frequency reaching 2 GHz," Opt. Express **15**(20), 13155–13166 (2007).
28. H. Byun, D. Pudo, J. Chen, E. P. Ippen, and F. X. Kärtner, "High-repetition-rate, 491 MHz, femtosecond fiber laser with low timing jitter," Opt. Lett. **33**(19), 2221–2223 (2008).
29. Batop sam-1550–6-x-2ps. (The use of product names is necessary to specify the experimental results adequately and does not imply endorsement by the National Institute of Standards and Technology.)
30. J. J. McFerran, W. C. Swann, B. R. Washburn, and N. R. Newbury, "Elimination of pump-induced frequency jitter on fiber-laser frequency combs," Opt. Lett. **31**(13), 1997–1999 (2006).
31. I. Coddington, W. C. Swann, and N. R. Newbury, "Coherent dual-comb spectroscopy at high signal-to-noise ratio," Phys. Rev. A **82**(4), 043817 (2010).
32. The detector and digitizer used are a thorlabs PDB110C and a Gage CS14200. (The use of product names is necessary to specify the experimental results adequately and does not imply endorsement by the National Institute of Standards and Technology.)
33. N. R. Newbury, I. Coddington, and W. C. Swann, "Sensitivity of coherent dual-comb spectroscopy," Opt. Express **18**(8), 7929–7945 (2010).
34. P. E. Ciddor and R. J. Hill, "Refractive index of air. 2. Group index," Appl. Opt. **38**(9), 1663–1667 (1999).

1. Introduction

The broad bandwidth and timing stability of femtosecond laser based frequency combs [1,2] has been a significant enabling technology for high precision distance measurements [3–16]. Cross-correlation and autocorrelation techniques [6–15] are especially able to exploit the broad bandwidth of femtosecond lasers for high precision. Dual-comb based techniques [11,12,15], a subclass of the cross-correlation techniques, are particularly attractive because they can scan an entire range window quickly allowing for rapid update rates against multiple targets, and requiring no balancing of interferometer paths. However, while the nanometer-level precision demonstrated by some of these systems could support future formation flying of satellites in space, it is excessive for many terrestrial applications where atmospheric effects generally limits optical distance measurements at the 10^{-7} level. Indeed, for many applications, such as machining, rapid update rates and simple robust technology are far more important than extreme precision. Here, we describe a dual-comb based LIDAR (light detection and ranging) system that greatly simplifies our previous demonstration [12], trading off the excessive nm-level precision for a significant reduction in hardware complexity.

The basic approach is shown in Fig. 1. As with applications of this technique to spectroscopy [17–21] or component characterization [22,23], the measurement is made by encoding information on a train of femtosecond pulses from the "probe" laser and then beating the probe laser with a second local oscillator (LO) laser operating at a slightly different repetition rate (see Fig. 1). In this case the encoding is done when the probe is retro-reflected off a target and reference surface to generate two co-propagating pulses separated by the time delay between the target and reference reflections. With each sequential pair of probe and LO pulses the relative pulse timing shifts slightly and a cross-correlation is formed in the

#151474 - $15.00 USD Received 21 Jul 2011; revised 22 Aug 2011; accepted 22 Aug 2011; published 7 Sep 2011

interference signal as the LO pulses "walk through" the probe pulses. For sufficiently stable femtosecond lasers this cross-correlation contains very precise information about the timing between the target and reference pulses; the pulse envelopes provide a time-of-flight range measurement while the carrier phase under the pulse provides an interferometric range measurement.

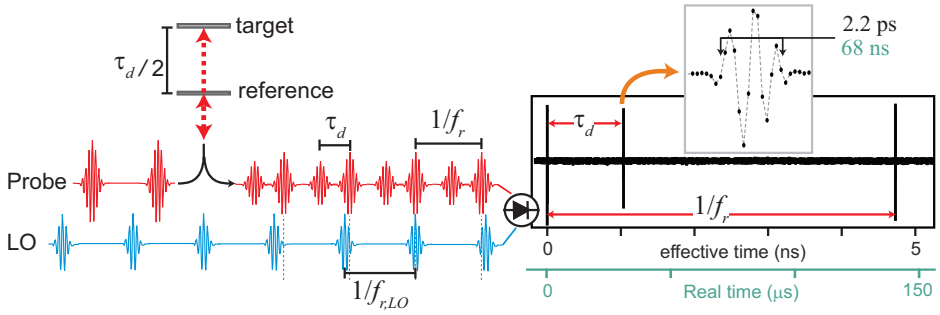

Fig. 1. Basic principle of dual comb LIDAR. Pulses from the probe laser are reflected off a target and reference plane and heterodyned against LO pulses at a slightly different repetition rate, $\Delta f_r = f_r - f_{r,LO}$, yielding the cross-correlation or interferogram, shown on the right for real data. This interferogram is repeated every 140 μs in real time corresponding to $1/\Delta f_r$. The interferogram can be interpreted as a down-sampled measurement of the probe pulse train, covering an effective time window of 4.8 ns, corresponding to the inverse of the 208 MHz repetition rate, and with effective time steps (visible in the insert) of $\Delta f_r/f_{r,LO}f_r$ = 160 fs, corresponding to the relative time advance between the LO and probe pulse train for each pulse. The temporal extent of the crosscorrelation in both real time (68 ns) and effective time (2.2 ps) is given to the right of the inset. These fine time steps allow for a precise measurement of the time duration between the reflection off the reference plane visible at zero time and the target plane visible at 1 ns (effective time) or ~35 μs (real time). The oscillations of the interferogram correspond to the difference between the effective carrier frequency of the probe and LO pulses (equal to the offset between probe and LO frequency comb teeth averaged across the spectra.)

Previous realizations of the setup, shown in Fig. 1, require the two laser combs sources to be fully stabilized with high residual coherence. In [12], we demonstrated just such a system with simultaneous time-of-flight and interferometric ranging to provide nanometer-level absolute ranging at a distance. The source stabilization can be achieved through active phase-locking [12], or through simultaneous measurements of the repetition rates and carrier frequencies combined with post-processing [19,21]. This full stabilization requires monitoring of four separate phase-lock signals (one each for the carrier and repetition rate for each laser) and leads to a complicated system. As we show here, we can dispense with all four of these high-bandwidth phase locks if one is only interested in the time-of-flight measurement, which can already provide sub-micron ranging. The requirements on the free-running laser are minimal and can be met by a sufficiently robust laser design. Specifically, we only require the relative free-running carrier phase be stable over the ~100 ns time scales required to construct a cross-correlation between two pulses and the repetition rate stable to better than 1 part in 10^7 over a few seconds. Moreover, we show that with a self-calibrating data analysis technique, it is sufficient to monitor the repetition rate of only a single laser. As compact ultrafast lasers are crucial for extending this technique to non-laboratory applications, we have also implemented this new system with the more robust passive mode-locking possible with saturable Bragg reflectors (SBR) [24–28].

The resulting overall ranging system thus reduces to two simple free-running femtosecond fiber lasers, a single digitizer, and a single frequency counter for calibration of the time axis. Despite this greater simplicity, we find a factor of three performance improvement achieving better than 200 nm precision within a 20 ms acquisition period at ranges up to a meter. The 200 nm precision is also sufficient to resolve the range ambiguity on a cw based interferometer at 1550 nm. Thus, if a higher resolution absolute distance measurement is

#151474 - $15.00 USD Received 21 Jul 2011; revised 22 Aug 2011; accepted 22 Aug 2011; published 7 Sep 2011

required one could achieve it by coupling this system with an equally robust CW interferometer [12].

2. Experimental setup

2.1 Laser design

The lasers employed here are an Erbium all fiber design operating at repetition rates (f_r and $f_{r,LO}$) 207.694 MHz and 207.687 MHz with a difference (Δf_r) of 7 kHz. The cavity design is a semiconductor saturable absorber mirror (SAM) based linear-cavity modeled loosely on [26–28] (see Fig. 2(a)). Each end facet of the fiber cavity is connectorized with a pc connector. One end of the laser cavity is formed by sandwiching a SAM [29] between the pc connector at the fiber end and a second pc connector. The output coupler at the other end of the laser cavity is similar formed by another pc connector coated with 35 nanometers of gold providing 90% reflection and 4% transmission. An intracavity polarizer simultaneously provides three functions: the polarization selectivity, an input channel for the 1480 nm pump light and a second slightly higher power output. As described in [30] the pump lasers are driven at or near full power to minimize pump noise and then optically attenuated to 100 mW. In this manner both femtosecond lasers can be driven off a single high power pump diode. An intracavity polarization controller provides some tuning of the laser output spectrum, which is centered at 1560 nm. The gain is provided by a 25 cm section of highly doped (80 dB/m) Er fiber with 8 μm core diameter. No free space section is required for either laser since the difference in the repetition rates can be precisely set by cutting and polishing down one of the cavity connector ends. As in [28] there is no attempt to balance dispersion beyond the normal dispersion of the SAM and the net cavity dispersion is anomalous. A PZT (piezo-electric transducer) stack, glued to the Er fiber, allows for slow tuning of the comb repetition rate. The lasers outputs are centered at 1560 nm and have a 6 nm FWHM (full width half max), Fig. 2(b).

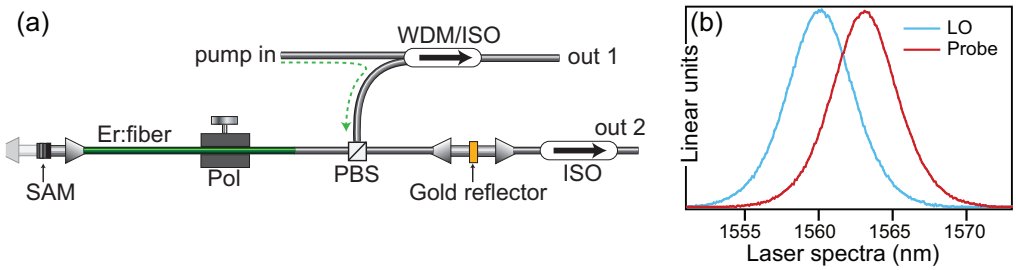

Fig. 2. (a) Linear cavity design for the 200 MHz fiber lasers. PBS-polarization beam splitter, Pol- polarization controller, ISO- isolator, WDM-wavelength division multiplexer. Output power was 2.0 mW from the PBS channel (out 1) and 0.4 mW through the gold reflector (out 2). (b) Spectra of the two lasers out of the out 1 port (port 2 is nearly identical). Spectral overlap could be improved in future designs but is not a significant limitation here.

2.2 Laser performance and suitability for dual-comb ranging

The all fiber design combined with the SAM makes for robust modelocked operation. In order to use these lasers in free-running operation for ranging measurements, we additionally require reasonable stability of both the carrier phase and repetition rates, as discussed below.

The Allan deviation of the laser repetition rates is shown in Fig. 2 and reaches 10^{-8} at one second (Fig. 3(a)). For the data presented in this paper there is a 2 second uncertainty in synchronization of the digitizer and the counters (limited by the precision of the digitizer timestamping). This leads to a $2\text{x}10^{-8}$ uncertainty in repetition rate and therefore range. While easily improved by more precise synchronization, this uncertainty is still comfortably below the 10^{-7} uncertainty imposed by air path fluctuations. If much higher precision was required, more rapid counter measurements could be implemented in addition to tighter synchronization. The similarity of the two lasers makes the 7 kHz difference in the two

#151474 - $15.00 USD Received 21 Jul 2011; revised 22 Aug 2011; accepted 22 Aug 2011; published 7 Sep 2011

repetition rates fairly immune to temperature changes. Note that this stability in repetition rate was achieved with no active temperature control of the lasers.

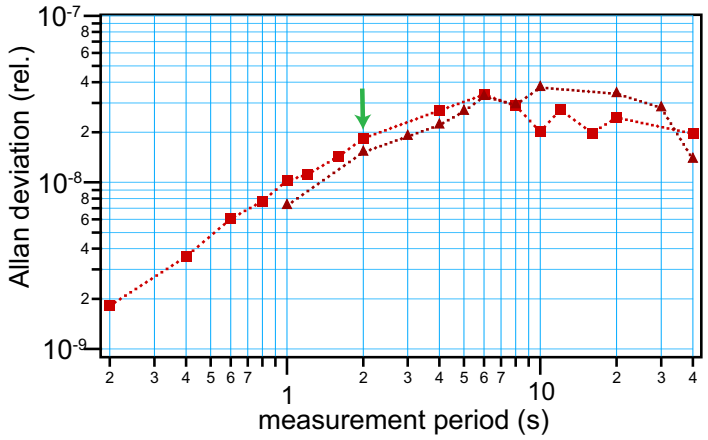

Fig. 3. Allan deviation of the free running Probe laser repetition rate measured with a 100 ms gate time (squares) and a 1 s gate time (triangles). The LO has slightly lower Allan deviation.

The time-of-flight measurement is derived from only the pulse envelope of the sampled interferogram; the carrier frequency is unimportant. We remove the carrier frequency through a Hilbert Transform of the signal. This operation has two requirements. First, the effective time steps, $\Delta f_r/f_{r,LO}\, f_r$, must be much less than the pulse width, $1/\Delta\nu$ to fully sample the signal. In real time, this requirement simply translates to requiring the rf spectrum of the interferogram have a width well below the Nyquist bandwidth of $f_{r,LO}/2$ = 100 MHz. We operate at Δf_r = 7 kHz so that the rf spectrum has a 10-dB width of 45 MHz (corresponding to an effective $\Delta\nu$ = 1.5 THz spectral overlap between the lasers). These Nyquist issues are discussed in more detail in [31]. Because the laser spectrum is so efficiently matched to the Nyquist range there is no need to amplify and filter the lasers as is done in [12].

The second condition for isolating the pulse envelope is that we require the relative carrier frequency between the two combs to be both stable over an interferogram and roughly centered in this 100-MHz Nyquist frequency window. Otherwise, there will be insufficient frequency separation between the pulse carrier frequency and the pulse envelope, the Hilbert Transform will fail, and the calculation of the pulse envelope will be distorted. This second requirement is also met by the free-running lasers as their carrier frequencies stay within 10 MHz over reasonable time windows. Moreover, the relative frequency is easily monitored through a Fourier Transform of the interferogram, and the lasers can be gently steered by adjusting the PZT or the current. This steering is on the minute timescale, rather than a sub-millisecond timescale required for a tight phase lock, and is easily accomplished through software control. In-phase/quadrature (IQ) detection offers an alternative solution by expanding the Nyquist window and greatly relaxing this constraint. Additionally, IQ detection would eliminate the need for a Hilbert transform thereby speeding the data processing. Yet another alternative is to use a balanced cross-correlator as in [13], which would eliminate this issue entirely.

2.3 Configuration of dual-comb interferometer

The system setup is depicted in Fig. 4 and strongly resembles those described in detail in [12,31]. The 2 mW output of the probe comb is passed through a 3 dB coupler acting as a circulator and is launched into the measurement path through a pc connector and collimating lens. The target is a glass wedge on a moving cart. The wedge is aligned so that the 4% reflection of the front face returns back down the measurement path. The 4% retroreflection off the pc coupler provides the reference reflection. The target and cart slide along a granite rail co-aligned with the measurement path. The measurement is validated against a

#151474 - $15.00 USD Received 21 Jul 2011; revised 22 Aug 2011; accepted 22 Aug 2011; published 7 Sep 2011

commercial HeNe based interferometer, which monitors the stage motion via a corner cube mounted to the back side of the wedge.

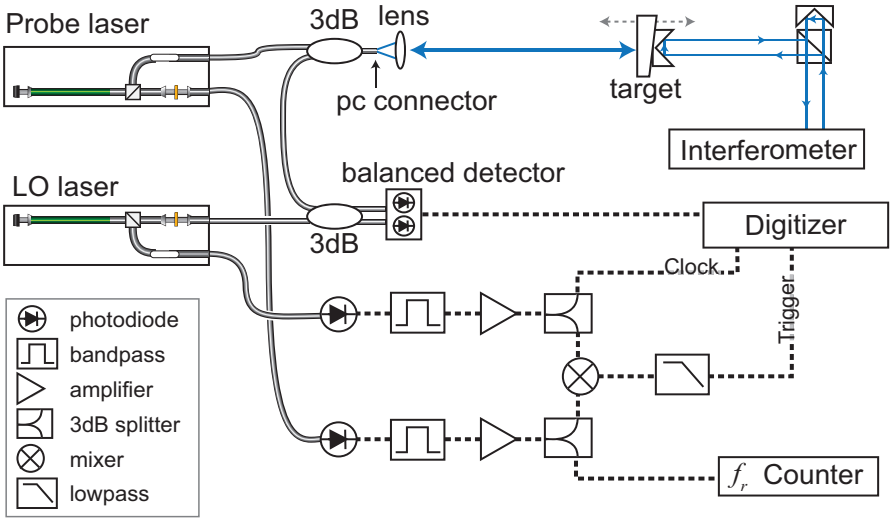

Fig. 4. Schematic of the setup. The two combs operate at 207.694 MHz and 207.687 MHz repetition rates providing a 7 kHz measurement update rate. The probe comb is retro-reflected off a pc connector and a movable glass wedge to form the measurement path. The overlap between the two reflected probe pulses and LO pulses is digitized synchronously with the LO comb pulses and stored for analysis. The counted probe pulse repetition rate provides the scaling for the distance measurements. (The effective LO pulse repetition rate is derived from the digitized signal itself.) The lasers were housed in a box to protect them from air currents, but no temperature control or active feedback was used to otherwise stabilize their output.

The retro-reflected probe pulses from the measurement path pass back through the 3 dB coupler and are combined with the LO pulses on a 100 MHz balance detector to perform the down-sampling against the LO. The fiber optical paths for the probe and LO differ by less than 4 meters of single mode fiber, so that the differential dispersion between the pulses is small compared to the inverse of their overlapping spectral bandwidth (which yields the ~1 ps full-width half-maximum interferogram signal shown in the inset of Fig. 1). The resulting signal is digitized by a 14 bit 200 MHz digitizer clocked at the LO repetition rate and recorded for analysis [32]. In addition, the 200-MHz repetition rate of the probe laser is counted on a 10 digit commercial frequency counter using a 1 second gate time. When the cross correlation signal is digitized the measurement is calibrated using the counter measurement closest in time to the digitizer time stamp, as described in the next Section. The LO repetition rate is not used in the processing but is mixed with the probe laser repetition rate and low passed filtered at 5 MHz to provide a 7 kHz Δf_r signal trigger signal. While this Δf_r signal is not strictly necessary it greatly simplifies the processing as it can force the reference peak to always occur at the beginning of the digitized signal.

The time domain signal-to-noise ratio (SNR), defined as the reference peak height relative to the baseline scatter, is 130 with the baseline noise arising in roughly equal parts from shot noise and detector noise. As is common in the dual comb approaches [33], our SNR is dynamic range limited by the detector. Increasing the power on the detector will increase the system SNR but leads to a saturation behavior that will distort the time domain signal and introduces a measurement systematic that drifts over a few second timescale and can be as large as 1 μm. To limit this saturation-induced systematic to below 200 nm we find that the power on the balanced detector must be attenuated to 10 μW/port or less (equal parts probe and LO). To compare, the specified cw saturation power of the detector is 70 μW.

#151474 - $15.00 USD Received 21 Jul 2011; revised 22 Aug 2011; accepted 22 Aug 2011; published 7 Sep 2011

2.4 Processing

An example of the raw recorded data was already shown in Fig. 1. The balanced interference signal between the two lasers shows a strong pulse for the reference reflection and a slightly weaker pulse for the target reflection. The entire window repeats every $1/\Delta f_r$ in realtime. This raw data is Hilbert transformed to generate the imaginary component of the complex analytic representation of the signal from the real part. The carrier oscillations (shown in the inset of Fig. 1) can then be removed by taking the modulus of this complex analytical signal to leave only the modulus, or signal envelope. The different pulses are then fit with a series of Gaussians to find the peak centers across the interferogram. (For these well-behaved spectra, a Gaussian fit was well matched to the observed shape; for more complex shapes that might, for example, arise for strong differential dispersion between the probe and LO pulses, a frequency-domain fit as in [12]. might be more appropriate). We identify a target and reference reflection and, for each interferogram, calculate the time delay between the target and reference pulse (Δ_{tr}) and the time delay between subsequent reference pulses (Δ_{rr}) both in units of the pulse sample number. The true time delay between the target and reference pulses, in effective time units, is simply

$$\tau_d = \left(\Delta_{tr} \Big/ \Delta_{rr} \right) T_r \tag{1}$$

where $T_r = 1/f_r$ is the counted repetition period of the probe laser. The time delay is then converted to distance using

$$d = \frac{1}{2}\left(v_g \tau_d + n v_g T_r \right) \tag{2}$$

where v_g is the group velocity derived from the Ciddor equation [34] based on measured temperature, pressure and humidity and n is an integer. The division by two is necessary to account for the folded geometry of the measurement path. The nv_gT_r term accounts for the ambiguity range; because the probe pulses repeat every $T_r = 1/f_r$, our range measurement is effectively aliased down by $(v_g/f_r)/2$ or 0.75 meters. If n is separately determined then this 0.75-m ambiguity can be removed, which is easily done in a number of ways. Here it is more than sufficient to do it by eye. One could also perform a second measurement while switching the roles of the probe and LO lasers as is done in [12] and extend the ambiguity range to ~20 km.

3. Experimental results

Figure 5(a) shows the Allan deviation for the target-to-reference distance at 1 m and continuous averaging times up to 2 s (the measurement limit set by our digitizer memory depth). At the minimum acquisition time of 140 μs, (set by the 7 kHz difference in laser repetition rates) the measurement precision is 2 μm and averages down as square root of time, dropping below 1 μm at 0.8 ms and below 200 nm at 20 ms averaging periods. At this precision, one might naturally handover to a cw interferometer for absolute distance measurement with no additional cost in averaging time. For this reason and because 200 nm is close to the 10^{-7} limit set by turbulence, the remainder of the data shown corresponds to a 20 ms averaging time.

Figure 5(b) shows the stability of the measurement over a longer, ~5 minute, period for a target at 0.6 meters. The 100 nm peak-to-peak scatter is within our expected precision from Fig. 5(a) for a 20 ms measurement window. These data demonstrate that the technique of self-calibration by use of counted probe laser repetition rate with a <2 sec synchronization error (e.g. Eq. (1)) does not introduce significant systematic uncertainty. (Over the same period the probe laser repetition rate drifted by 1 ppm.)

#151474 - $15.00 USD Received 21 Jul 2011; revised 22 Aug 2011; accepted 22 Aug 2011; published 7 Sep 2011

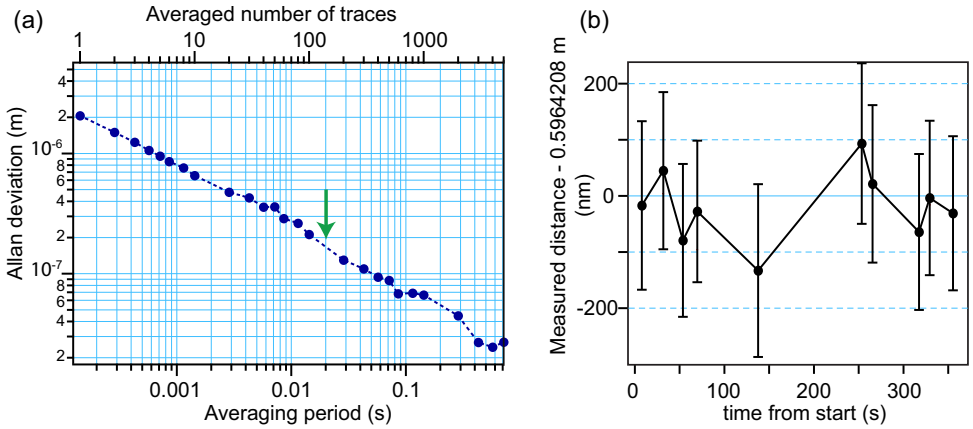

Fig. 5. (a) Measurement precision (Allan deviation) at a reference to the target range of 1 m. Precision at 140 μs is 2 μm averaging down as the square root of the averaging period and reaching 200 nm precision at 20 ms, indicated by the green arrow. (b) Long term stability test taken with a 20 ms averaging period and with the target positioned at 0.6 meters (black circles). Error bars are the standard deviation of the mean distance over the 20-ms period.

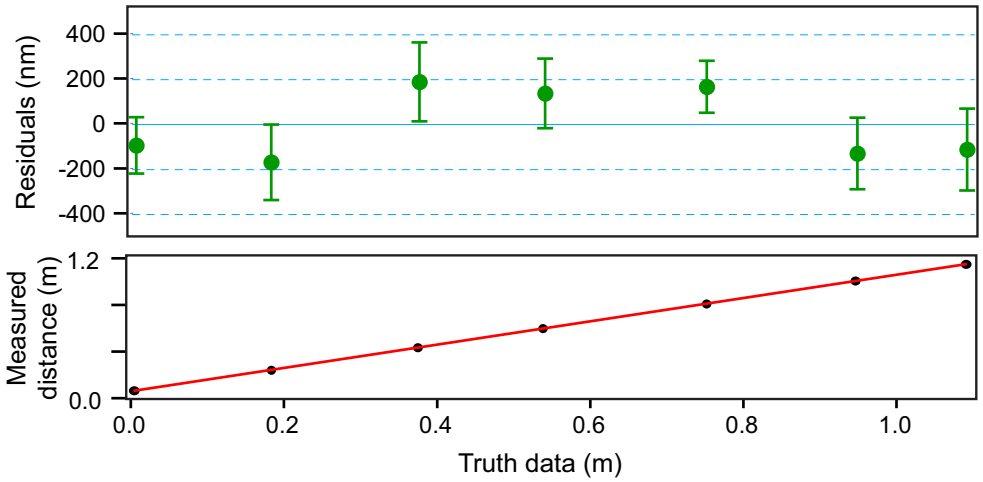

Fig. 6. Measured time-of-flight versus the commercial interferometer (truth data) and measurement residuals. The averaging period for the time-of-flight measurement is 20 ms. Error bars are the standard deviation of the mean distance over the 20-ms period. The measured distance has an offset from zero because the commercial interferometer zero is defined as the end of the granite rod while the dual comb system measures an absolute distance from the end of the pc launch connector, which is set back 59.7 mm from the edge of the rail.

To demonstrate the system linearity and absolute accuracy, we translated the target over the 1 meter granite rail and measured the distance to the target with our system and the cw interferometer shown in Fig. 4. Results are shown in Fig. 6. With a 20 ms averaging period the difference between the two measurements was within the expected 200 nanometers over the full 1 meter path difference. There is a slight "bowing" in the residuals, which is reproducible over multiple data sets and is likely caused by a slight twisting or bowing of our granite rail. Such a twisting would diversely affect the retro-reflected beam path used by the femtosecond lasers and the corner cube based path used by the commercial interferometer. Therefore, it is certainly possible that the system has slightly better than the 200 nm linearity shown here. In terms of absolute accuracy, while the commercial interferometer yields a very precise range measurement (~50 nanometers) the measurement is only a relative distance measurement and zero is arbitrarily defined as the end of the granite rail.

#151474 - $15.00 USD Received 21 Jul 2011; revised 22 Aug 2011; accepted 22 Aug 2011; published 7 Sep 2011

The use of a pc connector to define the reference plane has some disadvantages over the common path reference plane is used in [12] in that it is harder to define absolute distance since one must account for the optical path of the lens or carefully calibrate the system. On the other hand the pc connector is impossible to misalign and offers a significant advantage in term of robustness and stability. The ultimate choice of reference plane will likely depend on the application.

Measurement "dead zones" (e.g. "blind spots" where the range cannot be determined) in this experiment are small but do occur when the target and reference pulses overlap. Reference pulses occur every 5 ns in effective time (corresponding to the 0.75 m range ambiguity) and the target and reference pulses are separable as long as they are separated by 5 ps (in effective time – see inset of Fig. 1). This leads to a 0.1% dead zone or a 700 μm wide dead zone in every 0.75 m range window. While already small, this dead zone could be removed entirely by detecting the reference pulse on a separate detector at the cost of the introduction of an unknown time delay between target and reference pulses that would have to be calibrated out through a separate measurement.

5. Conclusion

We have demonstrated a dual comb range measurement technique with a high degree of both simplicity and precision. Range acquisition can be performed in only 140 μs with a precision of 2 μm. In as little as 20 ms, measurement precisions of 200 nm can be achieved. The linearity of the system has been demonstrated to be better than 0.2 ppm. The high update rates and meter-scale ambiguity ranges make this system potentially useful for manufacturing or machining applications where absolute distance measurement is needed.

As with [12] the system separately samples each range bin and is highly immune to stray reflections, which can lead to significant errors in cw interferometer system. Moreover the dual-comb system can be configured to monitor multiple targets, as long as the system is set up such that returning pulses from the targets do not overlap temporally. Similarly the system contains no slow scanning interferometer arms and minimal 0.1% dead zone in the range window, offering a significant advantage over systems based on matched interferometer paths.

Acknowledgments

This research was supported by the Bureau of Standards, Metrology and Inspection of the Republic of China (Taiwan), and by the National Institute of Standards and Technology. We would also like to acknowledge Bill Swann for technical support, Shelley Etzel and Kevin Silverman for depositing the gold coatings, and Paul Williams and Matt Kirchner for useful discussions. Work of NIST, agency of the U.S. Government and not subject to copyright.

#151474 - $15.00 USD Received 21 Jul 2011; revised 22 Aug 2011; accepted 22 Aug 2011; published 7 Sep 2011